

COMPARATIVE STUDY BY FEM OF THE STRESS AND STRAIN IN THE WORM GEAR REVERSE TAPERED PINION FOR DIFFERENT MATERIALS

Ligia Cristina BREZEANU¹, Bogdan BUCUR²

^{1,2} “Petru Maior” University of Tîrgu Mureș
Nicolae Iorga Street, no.1, 540088, Tîrgu Mureș, Romania

ligia.brezeanu@ing.upm.ro
bogdan.bucur@ing.upm.ro

Abstract

This paper presents a comparative study done by FEM of the state of stresses and strains of a worm face gear with reverse tapered pinion, worm wheel which is made of different materials: ERTACETAL C, BRONZE and CAST IRON.

The simulation of real physical phenomena engagement of screw-worm wheel is a sensitive issue that raises many problems. One of the methods allowing achievement of precise geometry of the structure would be considered as complete, is FEM.

Considering the geometrical complexity of the analyzed structure, proceed to a simplification of the phenomenon of contact between worm-worm wheels. Thus, for a correct interpretation of the studied phenomenon, corresponding geometric data from a section plane of worm-worm wheel gear is an analysis of the action momentary contact between the worm-worm wheels.

The theoretical evaluations are confirmed by the results obtained from the analysis and interpretation of experimental tests of the worm face gear with reverse tapered pinion studied.

Key words: Worm-Face Gear, Reverse tapered, FEM analysis, Finite Element, Stresses, Displacements

1. Theoretical aspects

The worm face-gear (Fig.1, Fig.3, Fig.5) belonging to the group of gears with cross axis is defined as a worm face-gear with reverse taper pinion.

Compared to the other gears [1], [8], [11]-[13] these face-gears present many constructive and functional advantages: increased bearing force to general-purpose worm gear, which makes their overall dimensions sensitively smaller, the contact line offers incomparably higher coverage, there are good lubrication conditions, higher ratios, increased accuracy and quiet operation.

Due to the particular geometry of worm face-gear with reverse taper pinion [4], [6]-[7] - the flanks of worm being strongly asymmetric allows the absolute control of the backlash, the axial displacement of a worm or screw worm wheel.

The worm face gear is characterized by the fact that the angle of pressure on two sides of the worm is not symmetrical. The worm face gear can work in load bearing flanks on both sides of 10^0 and the 30^0 . This makes the component values of occurring forces

in gear not identical for the two cases, when the bearing flank is the 10^0 or 30^0 respectively.

It is recommended that the active flank be used, the flank angle of lower pressure, a condition ensured by appropriate choice of the sense of rotation

The characteristic geometry of the elements of a worm face-gear with reverse tapered are presented in Fig.7, Fig.8.

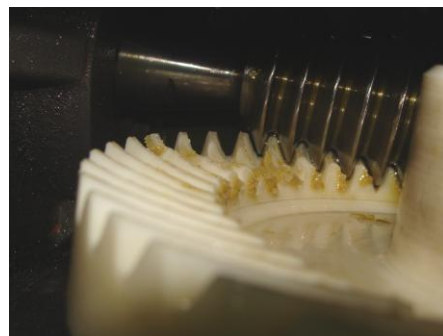


Fig.1: Gearbox with worm face gear with reverse tapered pinion - couple of materials: alloy steel-ertacetal C [4]



Fig. 2: Worm face gear with reverse tapered pinion
Couple of materials: alloy steel-ertacetal C [4]



Fig. 6: Worm face gear with reverse tapered pinion
alloy steel-bronze [4]

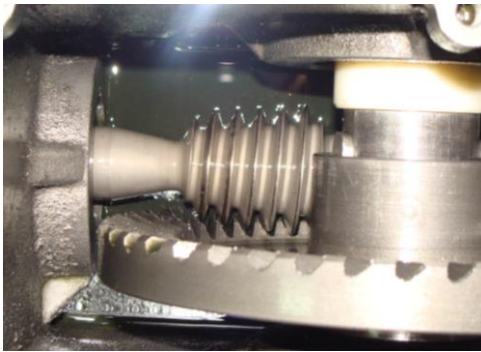


Fig.3: Gearbox with worm face gear with reverse tapered pinion - Couple of materials: alloy steel-cast iron [4]



Fig. 4: Worm face gear with reverse tapered pinion
alloy steel-cast iron [4]

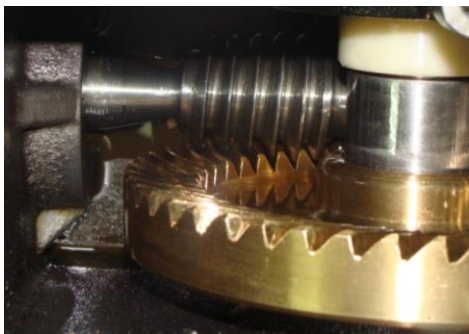


Fig.5: Gearbox with worm face gear with reverse tapered pinion - .Couple of materials: alloy steel-bronze [4]

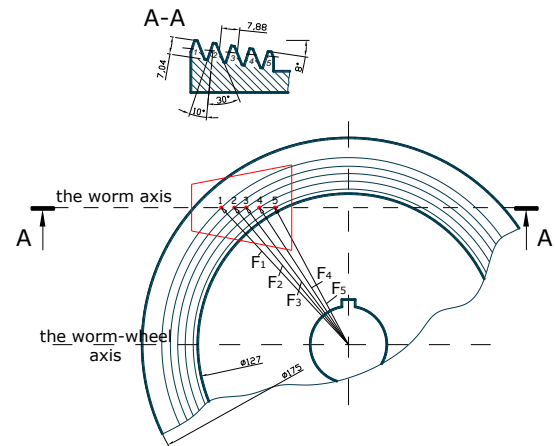
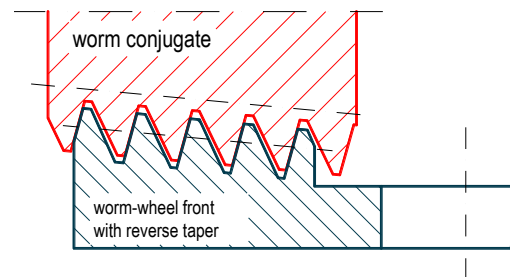


Fig. 7: The constructive geometry of worm face-gear.



The contact position of worm-wheel in operation

Fig. 8: Section through the worm worm-wheel the bearing flank 10°

2. Materials and Methods

2.1. FEM Analysis

2.1.1. Modeling and meshing

For FEM analysis of stress and strain state, having in mind the geometric complexity of studied structure [6]-[7], we have chosen between a tridimensional modeling [3], [9], [14] and a bidimensional one [2], which would result in a simplification of physical phenomenon of the contact between worm and worm wheel.

Accordingly to geometrical data from the plane of a section of worm-worm wheel gear (Fig.7.), an analysis of instantaneous action of contact between

worm and worm wheel in the plane of a section was made (Fig.8).

The modeling was made using Inventor 10 software [15] and then, for FEM analysis, the model was transferred in Algor V16 Fempro software (Fig.9.) [16].

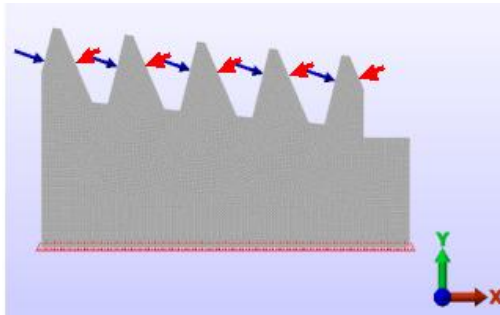


Fig. 9: Modeling – Meshing – Loads – Constraints

Finite elements used are type 2D – two dimensional quadrilateral and triangular. After meshing result:

- Number of nodes : 12989
- Number E.F.- type 2D: 13042

Nodal boundary conditions are fixed in the nodes of the worm-wheel.

The features of elastic material of wheel which is made of different materials of the worm wheel: *Ertacetal C*, *Bronze* and *Cast iron*, and properties described in Table 1 [5], [10], [17].

2.1.2. Loads

The flank loading was done by calculating the forces corresponding to the 5 points of contact between teeth of worm-wheel in contact with the conjugated surface of the worm (Fig.7.).

The torque transmitted of the worm-wheel M_t was calculated using the relations:

$$M_t = 9,55 \cdot 10^6 \frac{P}{n} [N.mm] \quad (1)$$

Which:

- P - power [kW];
- n - speed [rpm];

On the other hand the torque transmitted M_t is:

$$M_t = F \cdot \frac{d}{2} \quad (2)$$

Which:

- F - force in contact point of worm-worm-wheel [N];
- d - diameter of contact point corresponding for each tooth of the worm wheel [mm];

Thus, considering the diameter of contact points of five teeth of worm-wheel, the values of forces acting on the contact points are: $F_1 = 120.62$ N; $F_2 = 126.44$ N; $F_3 = 131.87$ N; $F_4 = 137.95$ N; $F_5 = 145.03$ N.

For constructive and functional reasons, tooth five is considered a hard drive smaller force than that calculated, namely: $F_5 = 130.5$ N.

2.1.3. Mechanical properties of the materials

Table 1 - Mechanical properties of the materials used for modeling

Mechanical properties of materials	Materials		
	Cast iron	Bronze	Ertaceta 1 C
Young's modulus E [GPa]	83÷170	96÷120	3.1
Poisson's ratio μ	0.2 ÷ 0.3	0.34	-
Yield stress [MPa]	100÷750	120÷300	68
Ultimate stress [MPa]	150÷1000	350÷630	-
Allowable stress compression / Allowable stress tension	2.5	1	-

2.1.4. The characteristic geometry of the worm face-gear with reverse tapered

Considering the following experimental values, corresponding to the experimental stand used (gearbox with worm-worm wheel) (Fig.1., Fig.3, Fig.5.):

- *power*: $P = 1,5$ kW;
- *speed*: $n=1500$ rpm input speed, output speed 32 rpm,
- *gear ratio*: $i = 1:47$;
- *axial distance*: $A=58$ mm;
- *the module*: $m=2,5$ mm;
- *bearing flank angle* : $\alpha_1 = 10^\circ$, *support flank angle* : $\alpha_2 = 30^\circ$;
- *Archimedes worm type taper*: $\delta_1=5^\circ$, reverse tapered worm wheel drive $\delta_2=8^\circ$

3. Results

The results are considered to be significant for the interpretation and relevance given the phenomenon studied, are the values:

- Equivalent stress Von Mises σ_{ech} ;
- Minimum principal stress σ_2 (with compression effect);
- Resultant structure shift; Displacement.

They studied four cases of loading:

- *Case I* - load bearing flank to 10° : loading in operating
- *Case II* - load bearing flank to 30° : loading in operating

On the simulations performed were obtained the following results:

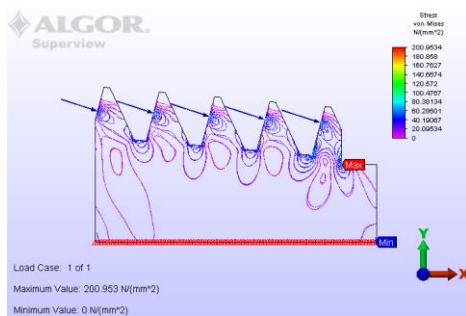
3.1. Stresses

- Stress distribution on the gear teeth, respectively Von Mises equivalent stress (σ_{ech}) and minimum principal stresses (σ_2) and displacements resulting (δ), is similar for all three cases considered, for either

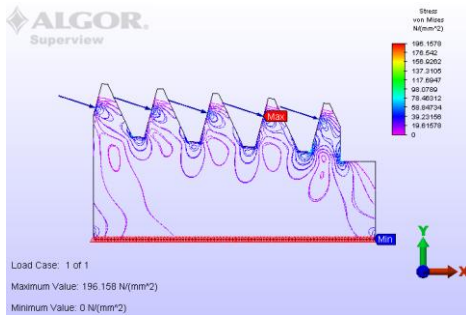
load bearing flanks of 10^0 and 30^0 , maximum stress on the flanks in contact with the flanks unsolicited show decreasing values (Fig.10., Fig.11., Fig.12., Fig.13., Fig.14., Fig.15., Fig.16., Fig.17.);

⇒ The worm wheel behavior, regardless of what material it is made from, is similar;

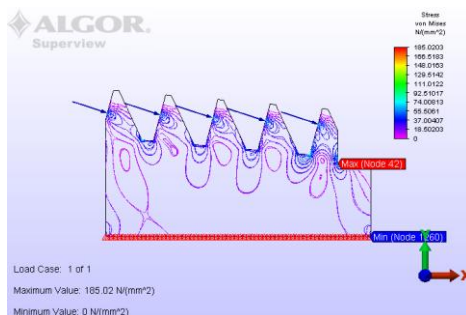
- The minimum principal stresses (σ_2); the given request forces on the flanks of the teeth, corresponding in operation is actually perpendicular to the tooth flank by compression;
- The maximum stress is produced in contact points of between the worm and worm wheel teeth, and the teeth of worm, the teeth are stress concentrators;
- The highest stress in load operation is produced in all cases considered of the last two teeth on the 4th instead of driving force and 5th in the base of the tooth (Fig.10., Fig.11., Fig.16., Fig.17.);



Ercetal C



Bronze

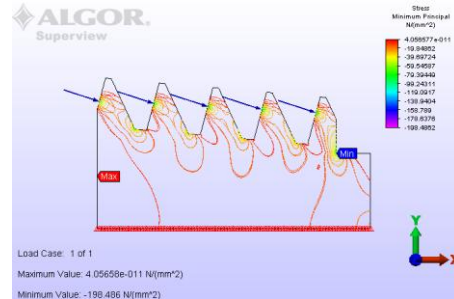


Cast iron

Fig. 10: Von Mises equivalent stress σ_{ech} on the bearing flank to 10^0

- One plausible reasons is that increasing the size of force of the last teeth is inversely proportional to the decreasing of the diameter where is situated the point of contact of the worm-wheel gear;

- The base of the tooth being machined in angle will always represent a stress concentrator;
- Loading of contact point was done by the nodal forces, the resulting maximum stress values directly nodal contact point, in fact contact between the worm-worm wheel is not punctual but is done on an area;
- The values of stress in the region nodes in the immediate neighborhood of the contact point are much smaller $\sim \sigma_{ef} \approx 150 - 200 \text{ N/mm}^2$, the situation is similar in all cases considered: worm wheel Ercetal C, Cast iron and Bronze;



Ercetal C



Bronze



Iron

Fig. 11: Minimum principal stresses σ_2 on the bearing flank to 10^0

3.2. Displacements

Distribution of the resulting displacements for all cases considered different worm wheel material: Ercetal C, iron, bronze, side loading and loading bracket 10^0 and 30^0 carrier side is similar, namely the maximum of first and last tooth is understandable given 1 and 5 lateral teeth rigidity lower than 2-3-4 middle teeth that are recessed and have a greater lateral stiffness (Fig.16., Fig.17.).

Table 2: Values of the equivalent stress Von Mises σ_{ech}

Values of equivalent stress Von Mises – bearing flank to 10^0					
σ_{ech}	117,43	122,22	127,39	133,11	126,02
	163,99	170,28	177,31	185,02	174,50
	173,68	180,48	187,95	196,16	185,13

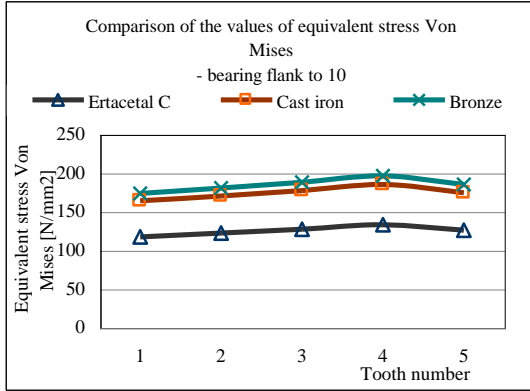


Fig. 12: Comparison of the values of equivalent stress Von Mises σ_{ech} for different materials of the worm wheel: Ertacetal C, Cast iron, Bronze

Table 3: Values of the minimum principal stress σ_2

Values of minimum principal stress –bearing flank to 10^0					
σ_2	-124,34	-129,15	-134,61	-140,59	-133,05
	-174,41	-180,71	-188,15	-196,22	-184,92
	-183,79	-190,58	-198,45	-207,01	-195,21

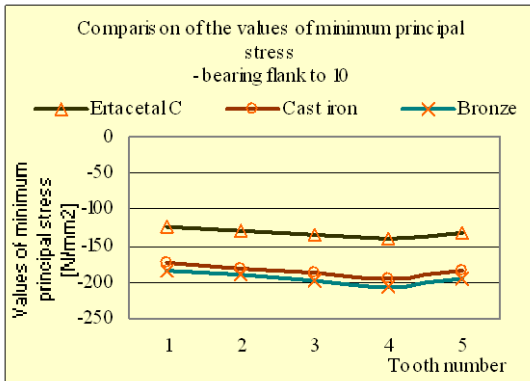


Fig. 13: Comparison of the values of minimum principal stress σ_2 for different materials of the worm wheel: Ertacetal C, Cast iron, Bronze

Table 4: Values of the equivalent stress Von Mises σ_{ech}

Values of equivalent stress Von Mises – bearing flank to 30^0					
σ_{ech}	88,73	93,66	96,26	99,08	100,62
	156,55	164,11	170,24	177,29	167,32
	165,86	173,46	180,45	187,99	177,62

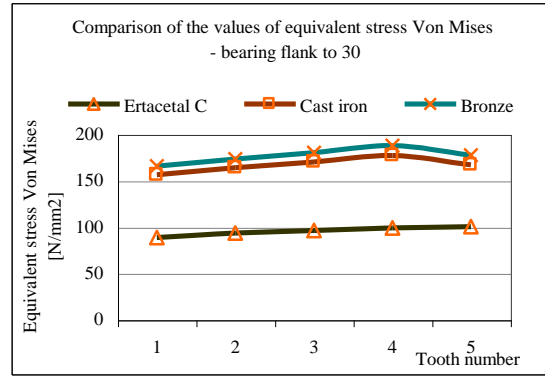


Fig. 14: Comparison of the values of equivalent stress Von Mises σ_{ech} for different materials of the worm wheel: Ertacetal C, Cast iron, Bronze

Table 5: Values of the minimum principal stress σ_2

Values of minimum principal stress –bearing flank to 30^0					
σ_2	-102,19	-107,88	-110,73	-113,85	-115,44
	-166,29	-173,14	-179,24	-186,38	-175,99
	-175,38	-182,69	-189,20	-196,81	-185,83

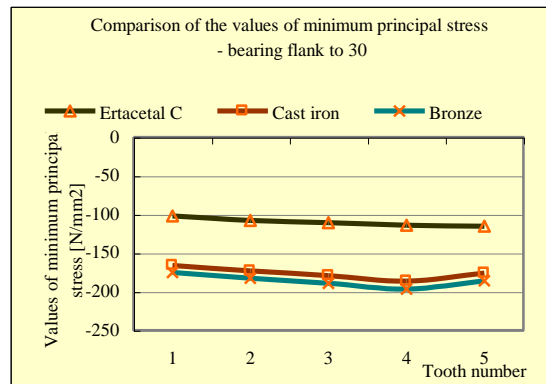


Fig. 15: Comparison of the values of minimum principal stress σ_2 for different materials of the worm wheel: Ertacetal C, Cast iron, Bronze

4. Discussion

Comparing the results of the simulations performed for the three situations in which the worm wheel is made of different materials: Ertacetal C, Cast iron and Bronze can be seen:

• The values of Von Mises equivalent stress (σ_{ech}) and principal stresses (σ_2) occurring across the main study are higher if worm wheel made of cast iron and bronze worm wheel than with concurrent of Ertacetal C;

• Considering, however, that the values of the strength characteristics of Ertacetal C is much lower than those of cast iron and bronze, the stress values developed under the same operating mode will cause the destruction of the worm wheel Ertacetal C ;

• The values of stress are similar for cast iron and bronze wheel, the stress are lower for cast-iron wheel;

➤ Given the strength characteristics of the materials studied [5], [10], [17], we can say that for the same geometry of the worm wheel and the same operating modes: $P=1.5$ kW and $n=1500$ rpm, although tensions overall study results are similar values for cast iron and bronze, Ertacetal C lower, *than a worm wheel is made by cast iron resists better operation than worm wheel made by bronze respectively Ertacetal C*;

➤ The worm wheel with the same geometry and the same operating modes: $P=1.5$ kW and $n=1500$ rpm, made of *material Ertacetal C will be destroyed at the flow entering shortly after the entry in operation*, its destruction will be produced corresponding to teeth 4 and 5, where the stress is maximum on the contact points of worm- worm wheel gear respectively the worm wheel teeth;

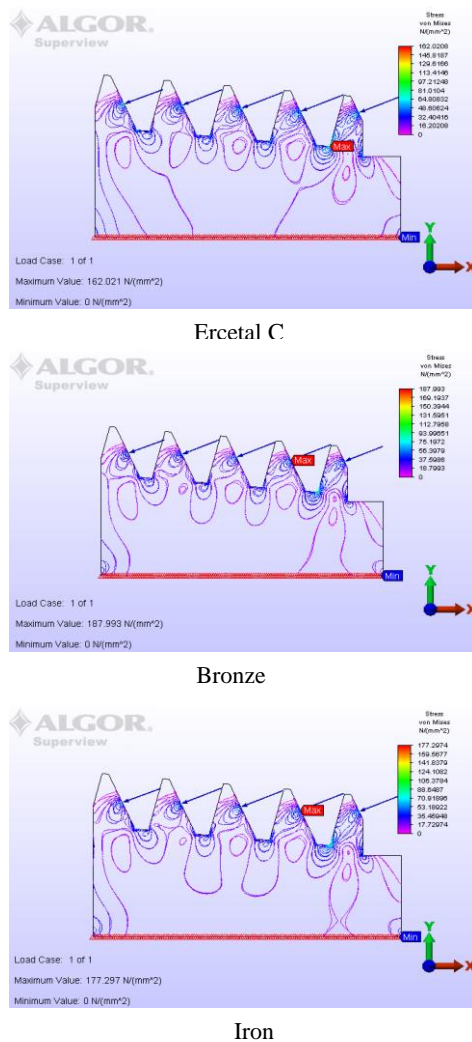


Fig. 16: Von Mises equivalent stress σ_{ech} on the bearing flank to 30°

5. Conclusions

In conclusion, we can say that for manufacturing of worm wheel we can use these materials: Ertacetal C, Bronze, Cast iron, with some clarifications:

➤ Regardless of the material used to prevent of the *phenomenon of stress concentration on the basis of teeth*, it is recommended to process with groove radius on the base of the teeth;

➤ Using a worm wheel made by Bronze or Ertacetal C would require reducing contact forces between the worm-worm wheel, that can be done by:

- Enlarging of the diameter of the worm wheel, leading to increased diameters which are contact points between te worm-worm wheel;
- Change the operating mode: reducing power $P=1.5$ kW or enlarge speed of $n=1500$ rpm;

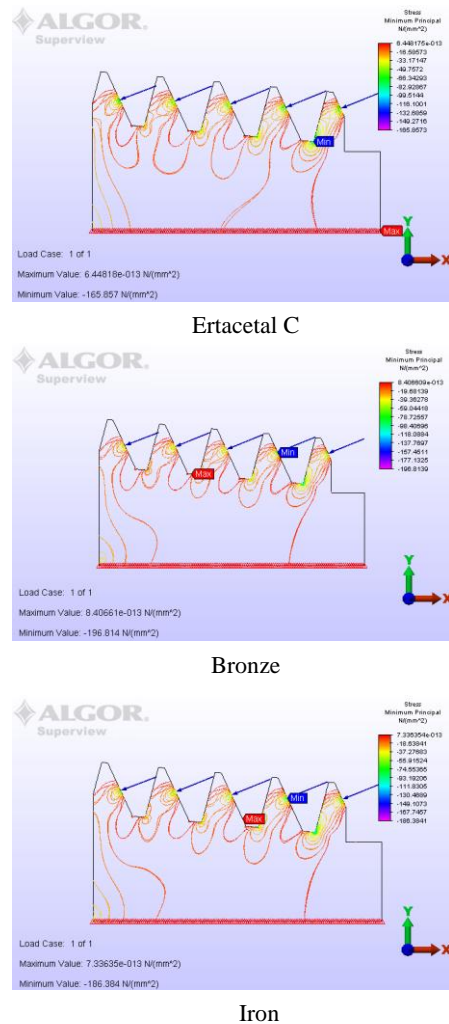


Fig.17: Minimum principal stresses σ_2 on the bearing flank to 30°

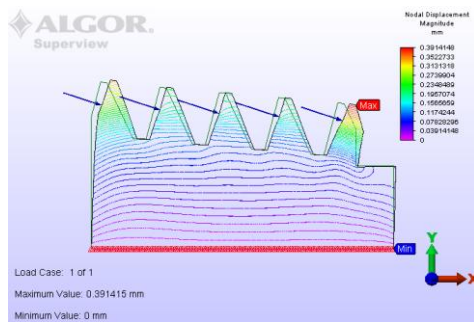
➤ A default resistance and greater durability in operation represented by the cast iron worm wheel;

➤ For medium load transmission and high precision, bronze is recommended, which gives a good reaction to lubrication;

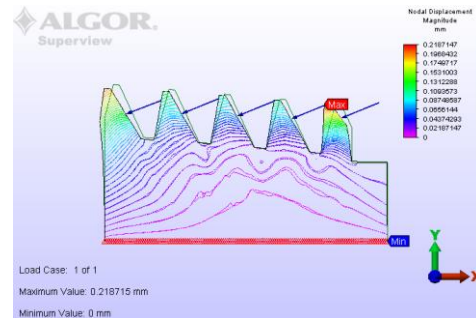
➤ For high transmissions through the worm wheel gears is recomanded process methods sintering or casting of non-ferrous materials;

- For application which require higher power transmission worm wheel the plastic injection process is recommended.
- A default resistance and greater durability in operation represented by the cast iron worm wheel; Fig. 18: Deformed position of structure. Displacements resulting δ - Loading on bearing flank to 10^0
- For medium load transmission and high precision, bronze is recommended, which gives a good reaction to lubrication;
- For high transmissions through the worm wheel gears is recommended process methods sintering or casting of non-ferrous materials;
- For application which require higher power transmission worm wheel the plastic injection process is recommended.

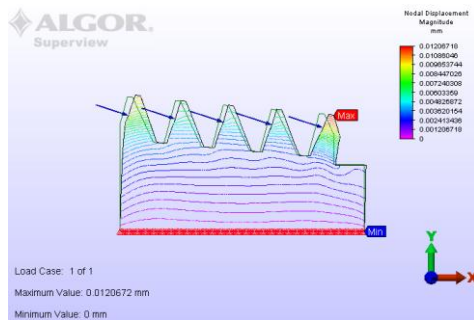
- For high transmissions through the worm wheel gears is recommended process methods sintering or casting of non-ferrous materials;
- For application which require higher power transmission worm wheel the plastic injection process is recommended.



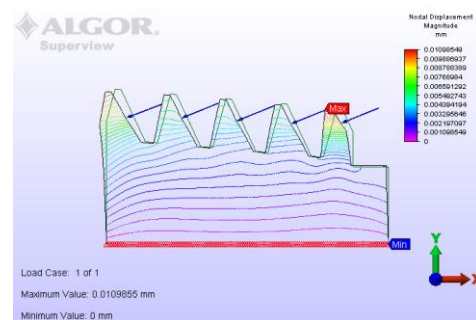
Ertacetel C



Ertacetel C



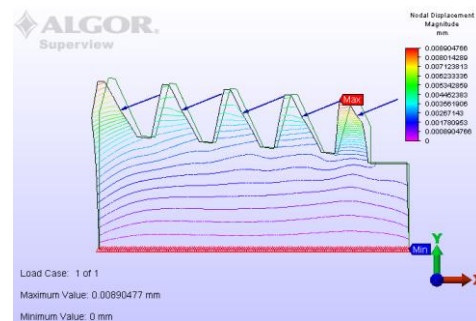
Bronze



Bronze



Cast iron



Cast iron

Fig. 18: Deformed position of structure. Displacements resulting δ - Loading on bearing flank to 10^0

Fig.19: Deformed position of structure. Displacements resulting δ - Loading on bearing flank to 30^0

- For medium load transmission and high precision, bronze is recommended, which gives a good reaction to lubrication;

References

- [1] Bohle, F., (1995), *Spiroid Gears*, Machinery, vol.62, pp.155-161;
- [2] Bolos, C., Brezeanu, L.C., (1998), *Analysis of stress in the tooth of spiroid worm*, in Proceedings of the 18-th Symposium on Experimental Mechanics of Solids, Jachranka, Warsaw, Poland, pp.164-168;
- [3] Brezeanu, L., C., Mathe, M., (2000), *The Study of the Influences of Cutting Forces on the Edge of Fellow's Cutters through Finite Element Method*, ISI Proceedings of the International Conference on Gearing, Transmissions, and

- Mechanical Systems, Professional Engineering publishing, Nottingham, U.K., pp.921-928;
- [4] Bucur, B., (2012), *Research concerning the geometry and technology of toothing the worm face-gear with reverse tapered pinion*, Ph.D. Thesis, Technical University of Cluj-Napoca, Cluj-Napoca, Romania;
- [5] Buzdugan, Gh., M. Blumenfeld, M., (1979), *Calculul de rezistentă al pieselor de masini/Strength calculation of machine parts*, Technical Edition, Bucharest, (in Romanian);
- [6] Georgiev, A.K., (1966), *Ortogonal worm-bevel gearing*, U.S. Patent 3289489;
- [7] Goldfarb, V.I., Trubachov, E.S., (2002), *Development and Application of Computer-Aided Design and Tooth Contact Analysis of Spiral-Type Gears with Cylindrical Worms*, AGMA-Technical Paper 02FTM2;
- [8] Litvin, F.L., Fuentes, A., Zanzi, C., Pontiggia, M., Handschuh, R., (2002), *Face-gear drive with spur involute pinion: geometry, generation by a worm, stress analysis*, Computer Methods in Applied Mechanics and Engineering, Vol. 191, pp.2785-2813;
- [9] Pathan, A., Prajapati, P., Patel, V.D., (2012), *Using FEM method stress and strain state analysis of the spur gear pair*, International Journal of Advanced Engineering Research and Studies, IJAERS, Vol.I, pp.44-47;
- [10] Pissarenko, G., Yakovlev, A., Matveev, V., (1979), *Aide-mémoire de résistance des matériaux/Help-memory, strength of materials*, Edition MIR, Moscow, (in French);
- [11] Simon, V., (1996) *Stress Analysis in Worm Gear Drive with Ground Concave Worm Profile*, Mechanism and Machine Theory, Vol. 31, No.8, pp.1121-1130;
- [12] Qin, D., Yang, H., Zhang, G., (2001), *Tooth contact analysis with generating surfaces*, International Journal of Gearing and Transmissions, Nottingham, UK, Issue No.3, pp. 29-35;
- [13] Yng, F., (2000), *Numerical Analysis and Three Dimensional Modeling of worm Gearing with Localized Tooth Contact*, Ph.D. Thesis, Nottingham Trent University, Nottingham, UK;
- [14] Wang, J.D., I.M. Howard, I.M., (2006), *Error analysis on finite element modeling of involute spur gears*, Journal of Mechanical Design, Vol.128, pp.90-97;
- [15] ***Autodesk INVENTOR (2004), *Professional, FEA Module*, CAD-FEM GmbH;
- [16] *** ALGOR, (2004), *Finite Element Analysis in Practice- Instructor Manual*, Pittsburgh, PA;
- [17] *** Ertacetal C: [Online]. Available: <http://www.ptfe.ro/inc/poliamida.pdf>